

Off-fault deformation rate along the southern San Andreas fault at Mecca Hills, southern California, inferred from landscape modeling of curved drainages

Harrison J. Gray¹, Charles M. Shobe¹, Daniel E.J. Hobley², Gregory E. Tucker¹, Alison R. Duvall³, Sarah A. Harbert³, and Lewis A. Owen⁴

¹Cooperative Institute for Research in Environmental Sciences (CIRES) and Department of Geological Sciences, University of Colorado, Boulder, Colorado 80309, USA

²School of Earth and Ocean Sciences, Cardiff University, Cardiff CF10 3AT, UK

³Department of Earth and Space Sciences, University of Washington, Seattle, Washington 98195, USA

⁴Department of Geology, University of Cincinnati, Cincinnati, Ohio 45221, USA

ABSTRACT

Quantifying off-fault deformation (OFD) rates on geomorphic time scales (10^2 – 10^5 yr) along strike-slip faults is critical for resolving discrepancies between geologic and geodetic slip-rate estimates, improving knowledge of seismic hazard, and understanding the influence of tectonic motion on landscapes. Quantifying OFD over these time scales is challenging without displacement markers such as offset terraces or geologic contacts. We present a landscape evolution model coupled with distributed lateral tectonic shear to show how drainage basins sheared by lateral tectonic motion can reveal OFD rates. The model shows that OFD rate can control the orientation of drainage basin topography: the faster the OFD rate, the greater the deflection of drainage basins toward a fault-parallel orientation. We apply the model to the southern San Andreas fault near the Mecca Hills (southern California, USA), where drainage basins change in orientation with proximity to the fault. Comparison of observed and modeled topography suggests that the OFD rate in the Mecca Hills follows an exponential-like spatial pattern with a maximum rate nearest the fault of 3.5 ± 1.5 mm/yr, which decays to ~ 0 at ~ 600 m distance from the fault. This rate is applicable since the initiation of differential rock uplift in the Mecca Hills ca. 760 ka. Our results suggest that OFD in this 800 m study area may be as high as 10% of total plate motion. This example demonstrates that curved drainage basins may be used to estimate OFD rates along strike-slip faults.

INTRODUCTION

Strike-slip fault systems can release stress by two means: slip on a master fault, and off-fault deformation (OFD). OFD, here defined as permanent fault-parallel displacement at the surface (Gold et al., 2015), has been recognized along many faults, yet the controls on OFD are not well understood (Milliner et al., 2015). Neglecting OFD can lead to underestimation of slip rates, plate loading rates, and associated seismic hazard (e.g., Shelef and Oskin, 2010). There are two major hypotheses for the dominant control on OFD. The first holds that the occurrence and rate of OFD depend on the structural maturity of the fault system, with increased maturity and decreased geometric complexity leading to decreased OFD (Dolan and Haravitch, 2014). An alternative view is that the occurrence and extent of OFD depend on the underlying lithology. For example, weakly lithified sediments could be more susceptible to nonrecoverable plastic strain due to granular flow and porosity changes (Maltman, 2012). The former implies that OFD rates will decrease with time, whereas

the latter suggests they should be steady in the absence of strain hardening or softening, all else equal. To uncover the controls on OFD, measurements over a range of time scales are needed. OFD measurements over single-earthquake time scales using pixel-tracking methods show promise (Gold et al., 2015), as have longer term (10^6 yr) studies (Shelef and Oskin, 2010), yet measuring OFD over intermediate (10^2 – 10^5 yr) time scales remains challenging.

One approach is to use basin shape or trunk stream orientation as a proxy for the OFD at the surface (Goren et al., 2015). In strike-slip landscapes, lateral tectonic motions reorient drainage patterns through stream deflection and piracy (e.g., Duvall and Tucker, 2015). At the 100–1000 km scale, entire drainage basins can be rotated by plate motion (Hallet and Molnar, 2001; Castelltort et al., 2012) and this rotation can be used to quantify OFD (e.g., Goren et al., 2015). However, the geomorphic effects of OFD at the subbasin scale (10–1000 m) are not well known. This is a critical knowledge gap because the 0–1 km scale takes up most of the

OFD, and thus has significant implications for tectonic dynamics (Shelef and Oskin, 2010).

We develop a model of hillslope and channel evolution that incorporates OFD as distributed tectonic shear to understand and quantify the effects of OFD at the subbasin scale over geomorphic time scales. We use this model to address two questions. Can fault-parallel OFD produce a measurable deflection in the orientation of ridges and valleys within an area subjected to distributed shear? Does the model predict a systematic relationship between the OFD rate and the ridge and valley orientation, such that one could infer OFD directly from topography? To test these concepts, we apply the model to dextrally curved drainage basins in the Mecca Hills (southern California, USA) along the San Andreas fault (SAF; Fig. 1).

CURVED DRAINAGE BASINS AT MECCA HILLS, SAN ANDREAS FAULT

Our study focuses on dextrally curved drainage basins within the Mecca Hills in the Coachella Valley of southern California. Here drainage basin ridgelines and channels deviate from the regional fault-perpendicular trend toward a fault-parallel configuration with proximity to the fault (Fig. 1). The curved Mecca Hills drainage basins are ~ 100 m wide and extend as much as 700–800 m from the SAF trace. Basins on the southwestern side of the fault do not demonstrate curvature. The northern part of the field area is bracketed by the northeast-dipping Skelton Canyon fault, which exhibits reverse faulting without lateral motion (Lindsey et al., 2014; McNabb et al., 2017). Because the fault is small near the border of our study area, and shows no evidence of lateral motion, we do not model it or consider it in our quantification of OFD rates. The basins are underlain by the weakly lithified to unlithified late Cenozoic fluvio-lacustrine silts of the Palm Spring Formation (McNabb et al., 2017). The presence of the Bishop ash in

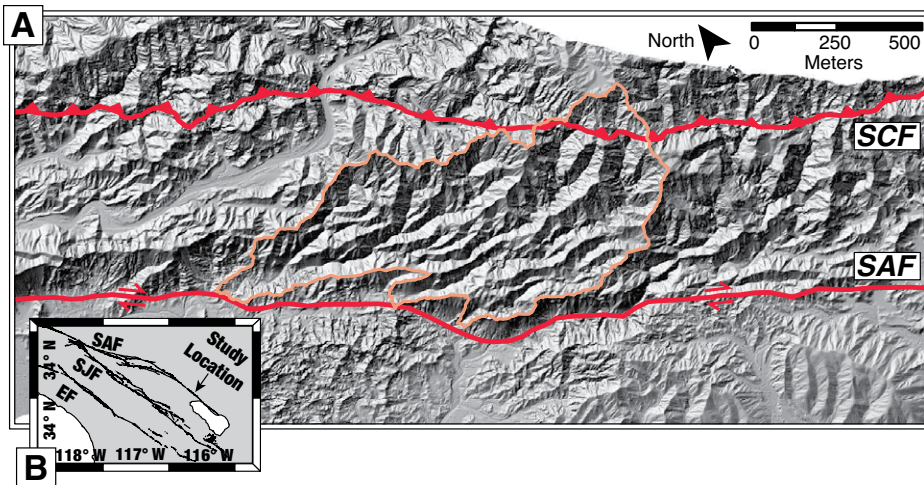


Figure 1. A: Drainages deformed by right-lateral motion on the San Andreas fault (SAF) near Mecca, California, USA. The center of the figure is $\sim 33.5925^{\circ}\text{N}$, 116.0050°W . Red lines indicate fault trace. Tan line indicates study area. SCF—Skeleton Canyon fault. Image is a lidar (light detection and ranging) hillshade (Bevis et al., 2005). **B:** Location of study area in southern California. SJJ—San Jacinto fault; EF—Elsinore fault.

regional stratigraphy implies that compression started after ca. 760 ka (McNabb et al., 2017) and that ongoing rock uplift is occurring due to transpression (Gray et al., 2014). We hypothesize that the dextrally curved basins result from OFD. To test the feasibility of this hypothesis, we develop a model of landform evolution under OFD, and compare its predictions with the observed topography in the Mecca Hills.

LANDSCAPE EVOLUTION MODELING

Following Duvall and Tucker (2015), we express landscape development and tectonic OFD using the equation

$$\frac{\partial z}{\partial t} = U - V(y) \frac{\partial z}{\partial x} - KA^{1/2}S + D\nabla^2 z, \quad (1)$$

where z is elevation, x is the fault-parallel direction, y is the fault-perpendicular direction, U is rock uplift rate (m/yr), V is the local lateral off-fault deformation or advection rate (m/yr), K is erodibility (1/yr), A is upstream drainage area (m^2), S is local slope (unitless), and D is hillslope diffusivity (m^2/yr). The first term in Equation 1 represents rock uplift relative to base level, the second represents lateral advection, the third is river incision, and the fourth is hillslope transport. Here, Equation 1 is appropriate given the cohesive but fine-grained local lithology, which avoids complications associated with the wear and transport of large clasts (Shobe et al., 2016; Glade et al., 2017). Here we assume that all fault-perpendicular shortening is accommodated via spatially uniform rock uplift. A full nondimensionalization and parameter space exploration of this model was given in Duvall and Tucker (2015); we modify that model by adding a definition of $V(y)$ that represents OFD:

$$V(y) = v_0 e^{-y/y_*}, \quad (2)$$

where V is the fault-parallel OFD rate relative to interior North America (m/yr), at distance y (m) away from the fault. The maximum off-fault displacement rate, v_0 (m/yr), occurs immediately adjacent to, but not on, the fault, and the characteristic length scale for deformation is y_* (m). In the model, y_* is chosen as the value (200 m) that recreates the width of the zone of curved terrain in the field area, and v_0 is obtained by finding the best-fitting model using geomorphic metrics described in the following. Note that v_0 is not the fault slip rate; rather, it represents the maximum deformation rate on the northeast side of the fault relative to a fixed North American datum.

Equations 1 and 2 are implemented on a rectangular grid using the Landlab 1.0 modeling toolkit (Hobley et al., 2017). Values for fluvial erodibility K and the hillslope diffusivity D are obtained from a full model parameter exploration and sensitivity analysis ($n = 480$)

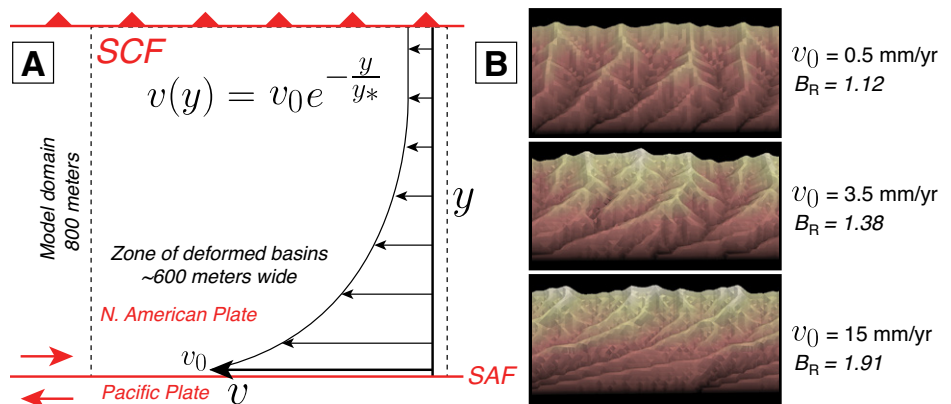


Figure 2. A: Definition diagram for the model described with Equations 1 and 2 in the main text. SCF—Skeleton Canyon fault; SAF—San Andreas fault; N.—North. **B:** Examples of modeled topography after 700 k.y. of simulated landscape evolution. Increasing off-fault deformation (v_0) rate leads to an increase in drainage basin curvature, which is reflected in the geomorphic metric B_R (see definitions in text).

minimizing misfit between the model and modeled total relief (200 m), mean elevation above base level (90 m), and basin reorientation index (1.38, discussed in the following) of the study landscape (Fig. DR1 in the GSA Data Repository¹). We find best-fit values of $K = 0.08 \text{ k.y.}^{-1}$ and $D = 0.02 \text{ m}^2/\text{k.y.}$ We use a rock uplift rate of 1.8 m/k.y. (Gray et al., 2014). The model produces curved basins that match the three landscape metrics and visually resemble those in the study area (Fig. 2).

We introduce a basin reorientation geomorphic metric (B_R) to compare observed and modeled topography. The B_R value is computed from digital terrain data following:

$$B_R = \frac{\text{total pixels with fault - subperpendicular aspect}}{\text{total pixels with fault - subparallel aspect}}, \quad (3)$$

where pixels with an aspect within $\pm 45^{\circ}$ of the fault strike are classified as subparallel; others are subperpendicular. We measure the B_R value for the study area using the B4 lidar data set (Bevis et al., 2005; Fig. 1), obtaining a value of 1.38 ± 0.02 . By contrast, modeled landscapes of the size of our study area (2 km wide and 0.8 km long) without any imposed OFD have B_R values of ~ 1.05 and catchments that do not appear curved.

To assess whether the model predicts a systematic relationship between curvature and deformation rate, we ran the model at various maximum deformation-rate values (v_0) and recorded the B_R value at each time step for 2 m.y. to collect statistically robust results. The modeled landscape demonstrates quasi-cyclic behavior in which OFD serves to increase the curvature of basins, whereas hillslope diffusion and stream piracy tend to straighten the channels

¹GSA Data Repository item 2018013, supplemental methods, and Movie DR1, is available online at <http://www.geosociety.org/datarepository/2018/>, or on request from editing@geosociety.org.

(Fig. 3A; Movie DR1). We count the number of time steps in which the model has a B_R value within the interval 1.38 ± 0.02 , and then divide this count by the total number of time steps. This number represents the likelihood that a model run with a given deformation rate will produce a B_R value comparable to that of our field area. This process is repeated for a range of OFD rates to obtain a likelihood value associated with each rate. We fit the resulting likelihood values with a Rayleigh distribution to estimate a mean and standard deviation for our deformation-rate estimates (Fig. 3B). The distribution implies a most probable OFD rate of 3.5 ± 1.5 mm/yr. We assume that development of the curved basins began concurrently with local rock uplift after 760 ka (McNabb et al., 2017). Thus, our best-fit OFD rate at Mecca Hills is an average since the beginning of the mid-Pleistocene.

SAN ANDREAS DEFORMATION-RATE ESTIMATES

Origin of the Curved Basins

OFD appears to be the most likely process to form the curved basins. Duvall and Tucker (2015) found that an elastic strike-slip fault intersecting drainage basins can generate shutter ridges that divert streams; their results show that pure on-fault deformation does not lead to curved basins, instead limiting channel diversion to the fault trace. Strike-slip fault motion alone does not appear sufficient to create curved basins. Another possibility is that bedding layers produce curved basins. However, the underlying submember of the Palm Spring Formation is only weakly lithified and exhibits no evident bedding control on drainage structure, and exposures of this submember elsewhere

do not appear to control stream orientation. A final possibility is that the curved basins are a relic of an antecedent drainage network prior to the onset of uplift after 760 ka. While we cannot fully discount this possibility, the regional drainage pattern prior to uplift was orthogonal to the trace of the SAF as alluvial fans drained the upstream mountains (McNabb et al., 2017). It seems unlikely that the streams would divert from the direction of steepest descent, and such diversion is not observed in non-uplifted alluvial fans north of the Mecca Hills (Gray et al., 2014). The only remaining viable mechanism for formation of the curved basins is distributed tectonic shear, and the observed basin curvature is consistent with model predictions for distributed shear. We therefore interpret the curved basins in the Mecca Hills to be a consequence of OFD. If this interpretation is correct, it raises the question of whether modeling the curved basins yields a unique prediction of OFD rate. To address this issue, we conducted a model sensitivity analysis and calibration procedure, with the goal of identifying an OFD rate that provides the best match between observed and simulated terrain.

Model Sensitivity Analysis and Calibration

We conduct a three-dimensional parameter study consisting of 480 model runs over a wide parameter space to assess whether our values for K , D , and OFD rate represent a unique combination that describes the curved drainages. We systematically vary K , D , and v_0 , and compare misfit in time-averaged B_R , time-averaged mean elevation, and time-averaged total relief between the 480 model runs and the study landscape. Model results are sensitive to all three parameters, but we observe a coherent region

of the parameter space with uniquely low misfit. We find that $K = 0.08$ k.y.⁻¹, $D = 0.02$ m²/k.y., and $v_0 = 3.5$ mm/yr produce the minimum misfit between observed and modeled topography (Fig. DR1). We interpret the low best-fit diffusivity as reflecting the steep relief of the study site, which is characterized by narrow ridgelines (~3 m) and quasi-planar, heavily rilled hillslopes that are probably dominated by overland flow. This morphology is better represented by the water erosion term in Equation 1 than by the linear diffusion (soil creep) term, and therefore the optimization procedure identifies a low value for D . The most important result of the parameter sensitivity study is that the calibrated model adequately captures the characteristic relief and ridge-valley structure of the study area (Figs. 1 and 2), and yields a unique best-fit value for v_0 .

Model Applicability

The applicability of our model to a given landscape depends on (1) the appropriateness of an exponential function to describe the OFD profile, (2) the effectiveness of B_R , mean elevation, and total relief as metrics for the field site comparison, and (3) the presence of curved basins. For (1), the appropriateness of an exponential function to describe OFD has theoretical and empirical support. England et al. (1985) derived a model for crustal deformation treating the crust as a thin viscous sheet, which resulted in an exponential model. Nelson and Jones (1987) and Rahl et al. (2011) found that this exponential model explained their OFD measurements at the 30 km and 150 km scales, respectively. Shelef and Oskin (2010) noted that an exponential function described their OFD measurements at the 200 m scale and concluded from a review of the literature that a nonlinear displacement pattern is not unique to the location or scale of the faults involved. An alternative approach using elastic dislocation theory produces approximately linear displacement profiles at the scale of our field area that do not appear to produce curved basins (see the Data Repository). Although beyond the scope of this study, an exploration of the underlying OFD mechanisms presents an interesting avenue for future research.

For (2), our analysis relies on the assumption that the B_R metric is sensitive to basin curvature and OFD, but insensitive to other morphologic characteristics, such as aspect ratio. Comparison of model runs with different degrees of OFD demonstrates that B_R is sensitive to curvature and OFD rate (Fig. 3). Alternative metrics that we tested, such as basin angle, proved to be less robust. Moreover, sensitivity analysis shows that the B_R metric is insensitive to the basin length-width ratio, provided the ratio is greater than unity (most basins are typically ~3; see the Data Repository for details). Our analysis also assumes that drainage orientation in the Mecca

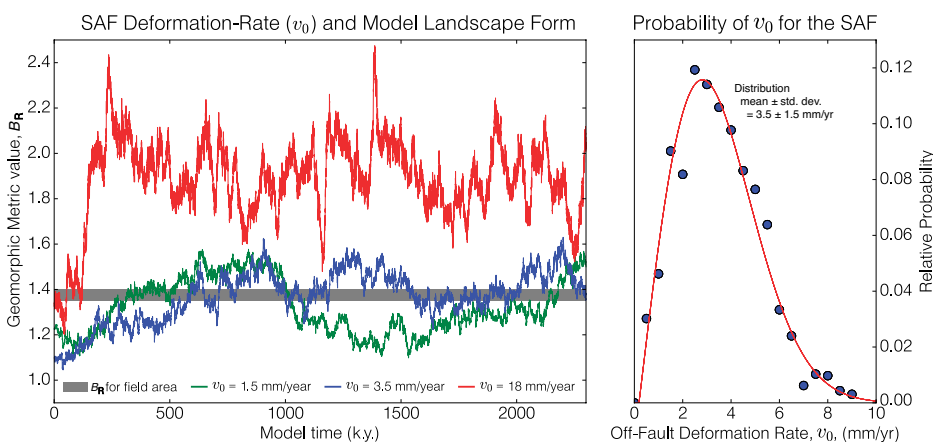


Figure 3. A: Basin reorientation geomorphic metric, B_R , plotted versus time for three different landscape simulations. Off-fault deformation (OFD) increases the B_R value, whereas stream piracy and hillslope diffusion decrease it. The landscape and metric reach a quasi-steady state wherein the B_R value varies around a mean. **B:** Relative likelihood that a model run with a given OFD rate will produce a B_R with the same value as the field area. Because of the B_R value variations, there is a probability that different OFD rates can produce the same landscape. Blue dots represent the relative likelihood that a model with given OFD rate matches the field area. Red line is a Rayleigh distribution fit to the data. We take the mean and standard deviation of the Rayleigh distribution fit of 3.5 ± 1.5 mm/yr as the most probable OFD rate.

Hills was perpendicular to the SAF prior to the onset of OFD, which is supported by field evidence, as discussed herein.

Model Implications

The smoothly curved topography in the field and our model results provides some clues to OFD mechanisms. OFD can occur in a range of styles, from pervasive shear to discrete faults to block rotation (Shelef and Oskin, 2010). Rotation of a block the size of the field area (700–800 m long) would lead to a linear displacement profile, which is inconsistent with the curvilinear drainage basin geometry of the Mecca Hills. How rotation of small blocks (~10–100 m long) would affect the landscape is unclear, but one possibility is that the creation of fault-perpendicular shear zones to accommodate small-block rotation would lead to fault-perpendicular drainage patterns as rivers preferentially erode the less-resistant zones between rotating blocks (e.g., Roy et al., 2016). A series of discrete parallel faults would be expected to produce a landscape with shutter ridge-like ridgelines and rectilinear channel networks (Duvall and Tucker, 2015), which are not observed in the Mecca Hills. A remaining option is pervasive continuous shear in which inelastic deformation is distributed across many submeter-scale faults. In this case, we would expect that a drainage network would progressively shear, creating the apparent ductile-like deformation pattern in the Mecca Hills area. Lithology is unlikely to be the main control on OFD in this location, as there are no curved basins northward along the SAF despite the occurrence of the same submember of the Palm Spring Formation. We conclude that pervasive continuous shear from a structural control remains the most probable primary control of the curved basins in our field site. The exact mechanism of structural control is not clear, but could be a wide shear zone in the underlying crystalline bedrock distributed into weakly lithified overlying sediments. There is a possibility that fault-perpendicular shortening has contributed to reorientation of the basins, which would cause our model to slightly overestimate OFD rates. However, we note that the SAF is oriented nearly parallel to the plate motion vectors and thus the effect of any shortening on topography is likely to be small compared to the lateral deformation.

Our results suggest that OFD may play a significant role in accommodating plate motion along the southern SAF. Generally, OFD can vary from 0% to 100% of the deformation rate of the main fault trace (Milliner et al., 2015). The 3.5 mm/yr of OFD measured across the 800 m study area accounts for 9%–10% of total plate motion (35–40 mm/yr) and is consistent

with distributed lateral motion across the region (Lindsey et al., 2014). Our values agree with the 9%–14% OFD at Durmid Hill, 30 km south-east along the SAF, based on stratigraphic data (Bürgmann, 1991). Our findings provide both evidence for a structural control on OFD and a new method that can obtain OFD data using topography. The model presented here should be generally applicable to locations where curved drainage basins are present along strike-slip or transpressional faults, which we suggest can be found where such faults uplift and/or crosscut weakly lithified sediments.

ACKNOWLEDGMENTS

This manuscript was greatly improved by reviews and feedback from Liran Goren, George Hilley, Nathan Toke, Olaf Zielke, Sarah Titus, Rich Briggs, Karl Mueller, and two anonymous reviewers. We thank editor James Schmitt. This research was supported by National Science Foundation grant EAR-1321735.

REFERENCES CITED

- Bevis, M., et al., 2005, The B4 project: Scanning the San Andreas and San Jacinto fault zones: American Geophysical Union Fall Meeting 2005, abs. H34B-01.
- Bürgmann, R., 1991, Transpression along the southern San Andreas fault, Durmid Hill, California: *Tectonics*, v. 10, p. 1152–1163, <https://doi.org/10.1029/91TC01443>.
- Castelltort, S., Goren, L., Willett, S.D., Champagnac, J.D., Herman, F., and Braun, J., 2012, River drainage patterns in the New Zealand Alps primarily controlled by plate tectonic strain: *Nature Geoscience*, v. 5, p. 744–748, <https://doi.org/10.1038/ngeo1582>.
- Dolan, J.F., and Haravitch, B.D., 2014, How well do surface slip measurements track slip at depth in large strike-slip earthquakes?: *Earth and Planetary Science Letters*, v. 388, p. 38–47, <https://doi.org/10.1016/j.epsl.2013.11.043>.
- Duvall, A.R., and Tucker, G.E., 2015, Dynamic ridges and valleys in a strike-slip environment: *Journal of Geophysical Research*, v. 120, p. 2016–2026, <https://doi.org/10.1002/2015JF003618>.
- England, P., Houseman, G.A., and Sonder, L., 1985, Length scales for continental deformation in convergent, divergent, and strike-slip environments: Analytical and approximate solutions for a thin viscous sheet model: *Journal of Geophysical Research*, v. 90, p. 3551–3557, <https://doi.org/10.1029/JB090iB05p03551>.
- Glade, R.C., Anderson, R.S., and Tucker, G.E., 2017, Block-controlled hillslope form and persistence of topography in rocky landscapes: *Geology*, v. 45, p. 311–314, <https://doi.org/10.1130/G38665.1>.
- Gold, R.D., Reitman, N.G., Briggs, R.W., Barnhart, W.D., Hayes, G.P., and Wilson, E., 2015, On-and off-fault deformation associated with the September 2013 Mw 7.7 Balochistan earthquake: Implications for geologic slip rate measurements: *Tectonophysics*, v. 660, p. 65–78, <https://doi.org/10.1016/j.tecto.2015.08.019>.
- Goren, L., Castelltort, S., and Klinger, Y., 2015, Modes and rates of horizontal deformation from rotated river basins: Application to the Dead Sea fault system in Lebanon: *Geology*, v. 43, p. 843–846, <https://doi.org/10.1130/G36841.1>.

- Gray, H.J., Owen, L.A., Dietsch, C., Beck, R.A., Caffee, M.A., Finkel, R.C., and Mahan, S.A., 2014, Quaternary landscape development, alluvial fan chronology and erosion of the Mecca Hills at the southern end of the San Andreas fault zone: *Quaternary Science Reviews*, v. 105, p. 66–85, <https://doi.org/10.1016/j.quascirev.2014.09.009>.
- Hallet, B., and Molnar, P., 2001, Distorted drainage basins as markers of crustal strain east of the Himalaya: *Journal of Geophysical Research*, v. 106, p. 13,697–13,709, <https://doi.org/10.1029/2000JB900335>.
- Hobley, D.E., Adams, J.M., Nudurupati, S.S., Hut-ton, E.W., Gasparini, N.M., Istanbuluoglu, E., and Tucker, G.E., 2017, Creative computing with Landlab: An open-source toolkit for building, coupling, and exploring two-dimensional numerical models of Earth-surface dynamics: *Earth Surface Dynamics*, v. 5, p. 21, <https://doi.org/10.5194/esurf-5-21-2017>.
- Lindsey, E.O., Fialko, Y., Bock, Y., Sandwell, D.T., and Bilham, R., 2014, Localized and distributed creep along the southern San Andreas Fault: *Journal of Geophysical Research*, v. 119, p. 7909–7922, <https://doi.org/10.1002/2014JB011275>.
- Maltman, A., 2012, *The geological deformation of sediments*: Dordrecht, Springer Science & Business Media, 362 p.
- McNabb, J.C., Dorsey, R.J., Housen, B.A., Dimitroff, C.W., and Messe, G.T., 2017, Stratigraphic record of Pliocene–Pleistocene basin evolution and deformation within the southern San Andreas fault, Mecca Hills, California: *Tectonophysics*, <https://doi.org/10.1016/j.tecto.2017.03.021> (in press).
- Milliner, C.W., Dolan, J.F., Hollingsworth, J., Lep-rince, S., Ayoub, F., and Sammis, C.G., 2015, Quantifying near-field and off-fault deformation patterns of the 1992 Mw 7.3 Landers earthquake: *Geochemistry, Geophysics, Geosystems*, v. 16, p. 1577–1598, <https://doi.org/10.1002/2014GC005693>.
- Nelson, M.R., and Jones, C.H., 1987, Paleomagnetism and crustal rotations along a shear zone, Las Vegas Range, southern Nevada: *Tectonics*, v. 6, p. 13–33, <https://doi.org/10.1029/TC006i001p00013>.
- Rahl, J.M., Brandon, M.T., Deckert, H., Ring, U., and Mortimer, N., 2011, Tectonic significance of ductile deformation in low-grade sandstones in the Mesozoic Otago subduction wedge, New Zealand: *American Journal of Science*, v. 311, p. 27–62, <https://doi.org/10.2475/01.2011.02>.
- Roy, S.G., Tucker, G.E., Koons, P.O., Smith, S.M., and Upton, P., 2016, A fault runs through it: Modeling the influence of rock strength and grain-size distribution in a fault-damaged landscape: *Journal of Geophysical Research*, v. 121, p. 1911–1930, <https://doi.org/10.1002/2015JF003662>.
- Shelef, E., and Oskin, M., 2010, Deformation processes adjacent to active faults: Examples from eastern California: *Journal of Geophysical Research*, v. 115, B05308, <https://doi.org/10.1029/2009JB006289>.
- Shobe, C.M., Tucker, G.E., and Anderson, R.S., 2016, Hillslope-derived blocks retard river incision: *Geophysical Research Letters*, v. 43, p. 5070–5078, <https://doi.org/10.1002/2016GL069262>.

Manuscript received 5 August 2017
Revised manuscript received 18 October 2017
Manuscript accepted 19 October 2017

Printed in USA